SATBAYEV UNIVERSITY

Engineering Journal of Satbayev University

Volume 148 (2026), Issue 1, 8-15

https://doi.org/10.51301/ejsu.2026.i1.02

Research into the ternary-remelted alloy Ti-10V-2Fe-3Al structural and technological properties

A.T. Mamutova[1], T.A. Chepushtanova[2*], B. Mishra[3]

[1]*Ust-Kamenogorsk Titanium and Magnesium Plant JSC, Ust-Kamenogorsk, Kazakhstan*
[2]*Satbayev University, Almaty, Kazakhstan*
[3]*Worcester Polytechnic Institute, Worcester, USA*

**Corresponding author: t.chepushtanova@satbayev.university*

Abstract. This paper presents the results of producing a triple-remelted Ti-10V-2Fe-3Al alloy. The results of SEM–EDS analysis of the alloy are reported, and the structure of the Ti-10-2-3 alloy along the height of an industrial electrode is determined. For the first time, results of a direct comparison between the morphology of the *α/β* phases and the local chemical composition in three characteristic zones of a 4.5 t electrode, "top", "middle 1", "middle 2", and "bottom", are obtained based on comprehensive SEM–EDS analysis. It is established that, with respect to the main alloying elements (Ti, Al, V), the ingot is fully chemically homogenized along its height, and the VAR (vacuum arc remelting) regime ensures an acceptable level of macrosegregation. It is shown that the concentrations of (Ti, Al, V), the principal alloying elements in Ti-10V-2Fe-3Al, do not change significantly between samples. SEM–EDS results indicate that the scatter in elemental concentrations is ≤1-1.5%, which is considered an indicator of high-quality VAR processing; this level of scatter implies minimal differences in elemental concentrations: Al variations are within ±0.5-1.0%, V variations are within ±0.5-1.0%, and Ti maintains a stable fraction of approximately ~83-86%. Morphological studies reveal that the *α/β* structure is formed uniformly, without pronounced columnar segregation. The results of the direct comparison of *α/β*-phase morphologies enabled the development of a quality-control methodology for electrodes based on SEM–EDS profiles.

Keywords: *titanium alloy; vacuum arc remelting; SEM–EDS analysis; triple remelting; α/β microstructure; morphology.*

Received: 18 November 2025
Accepted: 14 February 2026
Available online: 28 February 2026

1. Introduction

In recent years, research on titanium alloys has shifted toward detailed studies of the microstructural mechanisms that determine their performance characteristics, as well as the factors that affect the chemical homogeneity and phase state of industrially produced ingots. For the high-strength Ti-10V-2Fe-3Al (Ti-10-2-3) alloy, which belongs to the class of metastable *β*- and (*α*+*β*)-alloys, the distribution of alloying elements and the morphology of *α/β* phases after vacuum arc remelting (VAR) directly determine the strength, ductility, delamination resistance, and service life of critically loaded components. The primary methods for processing sponge titanium into ingots are vacuum arc remelting (VAR) and electron beam melting (EBM). These processes are the primary means of producing titanium alloys. VAR technology is widely used to improve the purity and structure of standard ingots, known as consumable electrodes, which are melted under vacuum.

Modern analytical approaches emphasize that not only the global chemical purity but also local microstructural inhomogeneities can significantly affect alloy properties. According to reviews on metastable *β*-alloys [1-4], even slight variations in the content of *β*-stabilizers (V, Fe), *α*-stabilizers (Al, O), or microsegregation of oxygen can lead to the formation of brittle zones, alter phase transformation kinetics, and cause the appearance of undesirable intermetallic phases, including α_2-Ti_3Al. Therefore, the importance of local analysis methods has increased in recent years, particularly scanning electron microscopy (SEM) combined with energy-dispersive spectroscopy (EDS), which enables the detection of micron- and submicron-scale structural inhomogeneities in industrially produced ingots.

A special focus within this group is the high-strength metastable *β*-alloy Ti-10V-2Fe-3Al (Ti-10-2-3), which has found wide application in chassis design, powertrain components, and integral fuselage assemblies due to its unique ability to achieve controlled *α*-phase morphology, regulated both by work hardening and aging regimes [5–7]. According to Banerjee & Williams [1] and Peters et al. [3] the mechanical properties of Ti-10-2-3 are determined by the distribution of *β*-stabilizers (V, Fe), the concentration of solid-solution elements in the *α*-phase (Al, O), the cooling rate, and the actual thermodynamic conditions of the *β*→*α* transformation.

Lutjering & Williams [2] and Boyer [8] emphasize that the spatial inhomogeneity of *β*-stabilizer distribution, local oxygen segregation, and *α/β* interphase morphology are critical parameters that determine fracture toughness, ductility, and the durability of highly loaded components.

post@uktmp.kz; t.chepushtanova@satbayev.university; bmishra@wpi.edu
Engineering Journal of Satbayev University. eISSN 2959-2348. Published by Satbayev University

Analyzing triple-melted ingots presents challenges, as a complex combination of factors influences structure formation: the composition and distribution of charge materials, solidification thermophysics, remelting conditions, and local temperature and heat flux variations. Large industrial electrodes weighing 4500 kg exhibit vertical and radial chemical gradients formed during ingot solidification, as well as differences in α/β-phase morphology between the top, middle, and bottom sections. These features are scarcely represented in the scientific literature: most publications focus either on laboratory melts or on structural analysis after heat treatment [9-12], while systematic SEM–EDS studies of large-scale, triple-melted industrial ingots are lacking.

The microstructure and performance characteristics of titanium alloys are determined by a set of phase transformations arising from titanium's pronounced polymorphism. Alloying elements introduced into titanium interact differently with the α- and β-phase lattices, stabilizing one modification over the other depending on changes in interatomic forces and their contributions to the thermodynamic stability of the phase states. This stability is defined by the polymorphic transformation temperature (PTT), a key parameter in the phase diagram of the Ti–X system [13].

Elements that predominantly dissolve in the α-phase, such as aluminum, oxygen, carbon, and nitrogen, increase the $\alpha\leftrightarrow\beta$ transformation temperature. Their presence leads to higher elastic moduli in the α solid solution and broadens its stability range. These elements, especially oxygen, nitrogen, and carbon, are inevitably introduced into the metal from both sponge titanium and alloying materials (C, Al) [14].

In contrast, β-type elements vanadium and iron lower the polymorphic transformation temperature, expanding the stability range of the β-phase. By dissolving in the β solid solution, they increase its elastic characteristics and promote the formation of a metastable β-matrix upon cooling. The transition of titanium atoms between β- and α-phases underlying these transformations is of particular interest.

Aluminum's low density reduces the alloy's specific weight and effectively increases its specific strength. It is a crucial α-stabilizer that provides strengthening while maintaining acceptable ductility. However, its content is limited by a critical threshold (~7 wt.%); exceeding this limit leads to the formation of the ordered intermetallic α_2-phase (Ti_3Al). The presence of this phase sharply reduces technological plasticity and impact toughness. To prevent α_2-phase formation, alloy compositions are optimized by limiting aluminum content and introducing β-stabilizers (Mo, V) [15].

Vanadium is the most versatile and widely used β-stabilizer in titanium alloys. Unlike other β-stabilizers, it simultaneously increases strength and ductility, making it unique among this group of elements. Its solubility in the α-phase reaches ~3%, allowing the development of alloys that combine the advantages of α-alloys (high weldability) and (α+β)-alloys (strengthening through heat treatment).

Oxygen, despite being an effective strengthener, significantly reduces ductility by forming a solid interstitial solution. At concentrations above ~0.2 wt.% and heating near the PTT, oxygen segregation at α-grain boundaries or the formation of fine α-phase particles enriched with oxygen may occur. These processes lead to a pronounced decrease in impact toughness and an increase in brittleness, consistent with [16-18].

Despite significant progress in theoretical modeling of β-alloys, data on the actual distribution of alloying elements and impurities in industrial triple-VAR ingots remain limited. Few studies provide a comprehensive correlation between α/β-structure morphology, chemical profiles, and local enrichment zones along the height of industrial-scale electrodes (mass 2.0-4.5 t), a crucial diagnostic aspect for ensuring VAR process stability and predicting the properties of the final semi-finished product.

This study aims to systematically investigate the structure and chemical homogeneity of an industrial Ti-10V-2Fe-3Al triple-VAR ingot using SEM–EDS, focusing on technologically induced inhomogeneities and identifying factors influencing α/β-microstructure formation along the electrode height.

2. Materials and methods

2.1. Initial materials

The object of this study was a triple-VAR Ti-10V-2Fe-3Al ingot, produced by vacuum arc remelting (VAR) according to the customer's specification: Al – 2.6-3.4%, V – 9.0-11.0%, Fe – 1.6-2.2%, O – max. 0.13%. The production of this ingot involved the following materials, whose chemical compositions are presented in Tables 1-5.

Table 1. Chemical composition of aluminum granules

Element	Al	Zn	Si	Fe	Mn	Mg	Ni	Pb	Sn	Ti	Cr	Cd	Be	Cu	C
Content, wt.%	99.8	0.003	0.025	0.113	0.02	0.0002	0.0051	0.001	0.0007	0.007	0.001	0.0001	0.0001	0.0004	0.002

Table 2. Chemical composition of the V–Al–Fe master alloy

Element	V	Al	Fe	B	C	Cr	Cu	Mo	P	S	Si	N	O
Content, wt.%	66.6	21.1	12.1	0.001	0.001	0.01	0.002	0.01	0.001	0.003	0.10	0.03	0.03

Table 3. Chemical composition of the V–Al–C alloy

Element	V	Al	B	C	Cr	Cu	Fe	Mn	Mo	Ni	P	S	Si	H	N	O
Content, wt.%	65.3	33.7	0.001	0.68	0.01	0.001	0.17	0.002	0.003	0.004	0.003	0.001	0.09	0.004	0.017	0.01

Table 4. Chemical composition of iron powder

Element	Fe	S	O(total)	N
Content, wt.%	99.98	0.003	0.019	0.001

Table 5. Chemical composition of titanium sponge

Element	Ti	Ni	Cl	O	N	Fe	C	Mn	Si	Mg	H	H_2O	Al	Sn	Cr	B
Content, wt.%	99.77	0.013	0.075	0.038	0.002	0.039	0.003	0.003	0.002	0.01	0.00062	0.01	0.005	0.002	0.017	0.001

2.2. Technology to produce titanium ingots in a vacuum arc remelting (VAR) furnace

The triple-VAR Ti-10V-2Fe-3Al alloy was produced on an industrial scale at Ust-Kamenogorsk Titanium and Magnesium Plant JSC. The VAR furnace configuration used for producing the Ti-10V-2Fe-3Al alloy is shown in Figure 1.

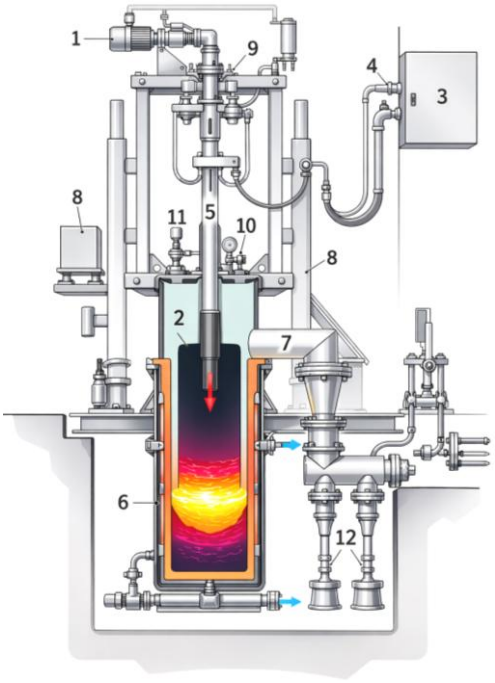

Figure 1. Schematic of the VAR furnace: 1 – electrode feed drive; 2 – furnace chamber; 3 – melting power supply; 4 – busbars and cables; 5 – plunger-type electrode holder; 6 – water-cooled jacket with mold (crucible); 7 – vacuum line; 8 – rotating column; 9 – coordinate positioning system; 10 – load cell system; 11 – TV camera system; 12 – oil booster pumps

During vacuum arc remelting (VAR), under the action of high temperatures generated in the electric arc zone between the consumable electrode and the base plate of the copper mold, the metal at the lower end of the electrode melts, and droplets of molten metal fall into the molten pool. Under the mold's cooling effect, an ingot is formed. Before the melting operation, the furnace chamber was evacuated, and vacuum was maintained throughout the melting process. Thus, molten metal droplets passed through a vacuum environment, ensuring deep purification of the metal from gases and certain nonferrous metal impurities and resulting in a dense ingot structure. Metal solidification in the water-cooled copper mold exhibited a clear directional character, aligned with the direction of heat removal. As a result of VAR, the mechanical properties of the metal improved and became more homogeneous in different directions of the ingot.

To reduce the risk of incorporating materials with excessively high or low density into the final product, the electrode holder was welded to the consumable electrode. The vacuum arc remelting process itself was carried out using separate melting assemblies. For this purpose, two molds were prepared: one intended for the electrode holder welding process and the other for the VAR process. Only molds and base plates that had undergone cleaning and drying procedures were used.

Using an overhead electric crane, the electrode holder was installed vertically at the upper end of the electrode, which was positioned in the melting assembly installed in the furnace. The electrode holder connected the ram (shaft) to the consumable electrode.

After furnace closure, the facility was evacuated. Leak testing was carried out in a computerized mode with data recorded in the process documentation. Upon reaching the specified vacuum parameters in the furnace chamber, a tight test was conducted.

The electrode holder was welded to the electrode by arc welding, forming an electric arc between the holder and the electrode's upper surface. Due to the arc energy, a molten titanium pool formed at the center of the electrode’s upper surface. Once enough liquid titanium had accumulated, the electrode holder was lowered using the electrode feed drive system and pressed into the molten pool. After solidification, a continuous welded joint was formed between the electrode holder and the electrode. This process was carried out under constant reduced pressure maintained by the VAR vacuum system.

After cooling the weld joint, the vacuum system was isolated from the furnace using appropriate vacuum valves, and atmospheric air was admitted into the furnace chamber.

The VAR operator loaded the starting material onto the bottom of the mold. This starting material was intended to protect the mold base plate from damage at the start of the melting process and was evenly distributed over the base plate, with a slight increase in thickness at the mold-base plate junctions. The furnace was then sealed and connected to the vacuum system.

The melting process was initiated from a remote control panel in the control room. Remelting process parameters were entered into the system.

During the melting process, monitored parameters were recorded in process logs every 20 minutes. A dedicated VAR operator performed monitoring and parameter adjustments at each processing stage.

After the melting was complete, the mold containing the ingot was removed from the furnace station using an overhead electric crane, transported to the assembly area, and placed on a special stand. The ingot obtained after remelting underwent dry cleaning of its lateral surface in a brushing machine. Subsequently, the ingot was transported to the “clean zone” of the machining area, where the crown was removed from the gating part on a lathe.

After crown removal, the ingot was subjected to high-pressure wet cleaning and drying in a washing unit designed for ingots and mold base plates. This stage completed the intermediate ingot processing procedure.

The electrode (first-remelting ingot) was installed with the gating part facing downward onto the base plate using an overhead crane. After installing the mold with the first remelting ingot into the melting station, the second remelting was performed. All subsequent processes associated with the second remelt vacuum evacuation, installation and welding of the electrode holder, preparation for melting, cooling, extraction, and mold washing were carried out following the same procedure as for the first remelt.

Surface treatment of titanium ingots was performed as a batch process in the machining area. Mechanical machining of the ingot end faces and lateral surfaces was performed on lathes. Machining was performed over the entire ingot surface until all surface irregularities and shrinkage cavities were removed entirely.

Sampling from titanium ingots was performed on a radial drilling machine by drilling using annular cutters. The number of samples, sampling locations, and dimensions of the sampling cones were determined in accordance with the applicable customer specification.

Sampling procedures, test methods, and testing volumes were conducted in accordance with the regulatory documentation for the product and the current technological and analytical control scheme. The quality, chemical composition, geometric dimensions, and weight of titanium ingots and alloys were required to comply with customer specifications.

The investigations employed scanning electron microscopy and elemental analysis using a JEOL JSM-7000 SEM equipped with EDS. Elemental composition was also determined by X-ray fluorescence analysis using an Olympus Element S XRF analyzer, and the alloys were chemically analyzed.

3. Results and discussion

3.1 Results of Ti-10V-2Fe-3Al alloy production

Vacuum arc remelting (VAR) of the Ti-10V-2Fe-3Al alloy was carried out in three successive remelts.

During the first remelt, the melted alloy mass (Δm) was 4.5 t, and the melting time (Δt) was 7 h 40 min. The electrode cross-sectional area (S_e) was 500 mm^2.

In the second remelt, Δm was 4.4 t and Δt was 10 h, with S_e equal to 600 mm^2.

The third remelt was performed with Δm = 4.4 t and Δt = 21 h 40 min, using an electrode with S_e = 680 mm^2.

The titanium density (γ_t) used in the calculations was 4.67-4.75 g/cm^3.

The calculated chemical composition of the consumable electrodes was identical for all melts and was as follows (wt.%): Al – 3.25; V – 9.70; Fe – 1.95; O – 0.105; C – 0.011.

The first remelt was performed in a mold with a 620 mm diameter. The first electrode was remelted at a mass melting rate of 9.90 kg/min, the second at 7.49 kg/min, and the third at 7.96 kg/min. Melting was carried out, resulting in a residual disk with a height of at least 40 mm.

Cooling after the first remelt was conducted for 10 h under residual pressure in the VAR furnace chamber (a key process parameter); cooling times for the second and third remelts were 10 h and 8 h, respectively. The average voltage during the steady-state melting stage ranged from 29.8 to 33.3 V, and the solenoid coil operated at a ±3 s periodicity.

The calculated composition of the titanium electrodes is presented in Table 6.

Table 6. Calculated charge composition of consumable titanium electrodes

Charge material	Melt 1, kg	Melt 2, kg	Melt 3, kg	Melt 4, kg
Al granules	17.1	17.1	17.1	17.1
V-Al-C master alloy	50	50	50	50
V-Al-Fe master alloy	588.3	588.3	588.3	588.3
TiO_2	8.2	8.6	8.7	8.6
Fe powder	16.4	16.5	15.7	15.4
Sponge titanium	3819.7	3819.4	3819.9	3820.3
Total	4500	4500	4500	4500

Thus, the Ti-10V-2Fe-3Al alloy was produced by triple VAR remelting. Subsequently, the alloy microstructure was investigated using scanning electron microscopy combined with energy-dispersive X-ray spectroscopy (SEM–EDS).

To study the alloy's composition and properties, four samples were taken from the electrode in the regions “top”, “middle 1”, “middle 2”, and “bottom” on the ingot's lateral surface. The results of the chemical analysis of the alloys are presented in the figure. The chemical composition of the surface samples from the four experimental Ti-10V-2Fe-3Al alloys meets the material specification. The scheme of dividing the alloys into sections is shown in Figure 2.

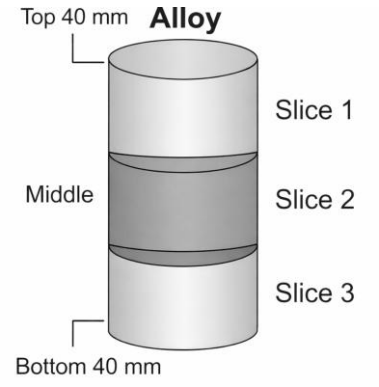

Figure 2. Scheme of alloy sectioning

Each experimental alloy was then divided into three sections, and samples were collected from the ends of each section for elemental distribution analysis across the alloy cross-section. The first cut was made 40 mm from the top of the ingot; the second, from the middle of the ingot as a representative sample of the steady-state melting regime; and the third, 40 mm from the bottom.

3.2. SEM-EDS results

To establish the relationship between the microstructure of Ti-10-2-3 titanium alloys and charge inhomogeneity, the type of alloying materials (V–Al–Fe, V–Al–C, TiO_2), the charge preparation method (briquetting, layered assembly), VAR melting regimes, and defects formed “from bottom to top” along the electrode height, SEM–EDS analysis was performed on the produced Ti-10V-2Fe-3Al alloy.

From a technological standpoint, the application of this method is also highly relevant, since industrial production may result in vertical (along the ingot height) and radial (from center to periphery) chemical gradients, non-uniform distribution of β-stabilizers (V, Fe), and variations in α/β-phase morphology during cooling. SEM–EDS analysis enables modeling of optimal technological conditions for ingot production and provides insight into the origins of these production-related issues.

The objects of investigation in the SEM–EDS analysis were four electrode zones: ingot samples taken from the “top”, “middle 1”, “middle 2”, and “bottom” regions.

The rationale for selecting these sampling locations was to investigate the following processes occurring within the ingot: the top-region sample was intended to identify potential defects associated with the final VAR pass; the middle-region samples were used to confirm steady-state crystallization; and the bottom-region sample was analyzed to reveal possible degradation of ingot structure resulting from interaction with the mold jacket or base plate.

For the SEM–EDS analysis, selected magnifications were used to characterize the structural features and phase distribution within the ingot, namely 500× for the overall micro-

structure and primary phase distribution, 1000-2000× for the α-phase plate morphology, and 5000× for local microstructural features, dispersed particles, and segregation zones.

Accordingly, the study focused on identifying vertical chemical gradients (V or Fe enrichment upward or downward), the distribution of *β*-stabilizers during remelting, the presence of oxygen or carbon segregation, an increase in oxygen content in the upper part of the ingot due to contact with residual gases during VAR, and oxygen enrichment at *α*-phase boundaries as an early stage of α_2-Ti_3Al formation.

3.2.1. Results of sample morphology analysis

As a result of studying the patterns of morphological evolution of the *α*/*β* structure, the following structural features were identified:

1). Top sample. At magnifications of ×3000-5000, thin, parallel, step-like layers, small, loose fragments, and isolated fine particles on the surface were observed. The EDS spectrum confirms the dominance of Ti (TiK*α* peak at ~4.5 keV), with pronounced peaks of V and Al and a noticeable fraction of C. The surface is relatively smooth, with isolated defects; however, the increased carbon content is attributed to the influence of the final stages of remelting, surface reactions, and/or polishing.

2). Bottom sample. At magnifications of ×3000-5000, distinct clusters of rounded and irregularly shaped particles accumulating between the "steps" of the matrix are clearly observed. By their morphology, these features resemble nonmetallic inclusions (oxides or slag fragments). Pronounced layering, significant defects, and a high number of nonmetallic inclusions were identified. This indicates that the structure formed during an unstable initial remelting stage, with possible non-uniform crystallization and local dendritic segregation, which is typical of the bottom region of an ingot. The EDS spectrum shows a Ti content of approximately 83.5-84 wt.%. The contents of V and Al are also close to nominal values, and no pronounced downward vertical segregation of *β*-stabilizers is observed. The carbon content is noticeably lower than in the top region, indirectly confirming the surface-related nature of part of the carbon enrichment in the upper section.

3). Middle 1 sample. At magnifications of ×3000-5000, individual *α*-plates appear more flattened and well-fused, and the surface is relatively smooth, without many porous particles. This region of the ingot exhibits the most uniform lamellar structure. It contains a minimal number of inclusions, indicating a steady-state VAR regime optimal for the formation of a homogeneous *α*/*β* microstructure. In this zone, the chemical composition is the most stable and closest to the calculated Ti-10V-2Fe-3Al system. The low carbon content and absence of pronounced oxygen peaks indicate a minimal presence of gas-saturated and oxide-related defects. Morphologically, this corresponds to the steady-state remelting region, where the *α*/*β* structure is uniformly formed without pronounced columnar segregation.

4). Middle 2 sample. At magnifications of ×3000-5000, this region exhibits a layered, fractured zone containing an oxide phase, with film-like or slag-related inclusions. The EDS spectrum indicates the formation of structural defects in this region.

Since the selected middle-region sample confirms a steady-state crystallization process, SEM–EDS analyses of this sample ("middle 1") are presented in Figures 3-5:

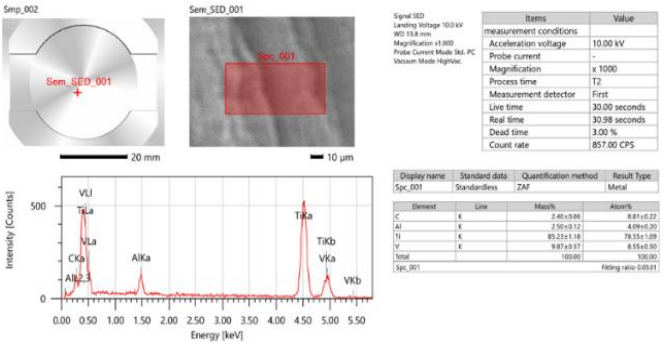

Figure 3. SEM elemental analysis results of the surface area of the "middle 1" sample

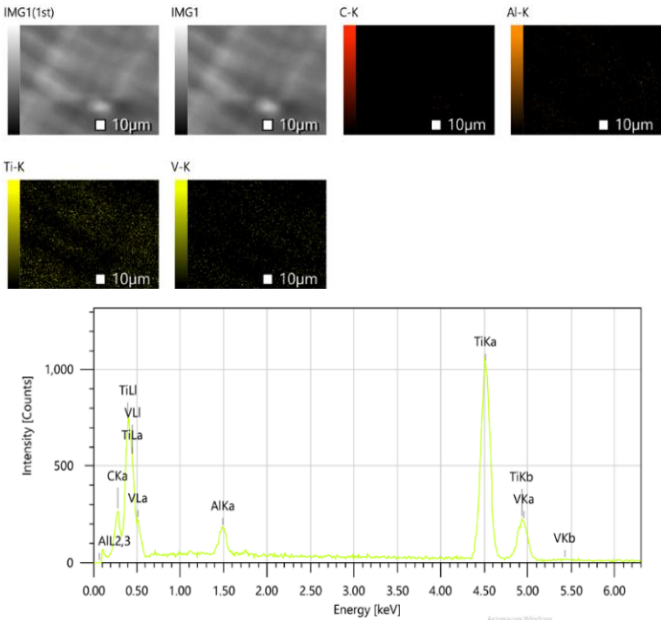

Figure 4. EDS mapping results of the "middle 1" sample

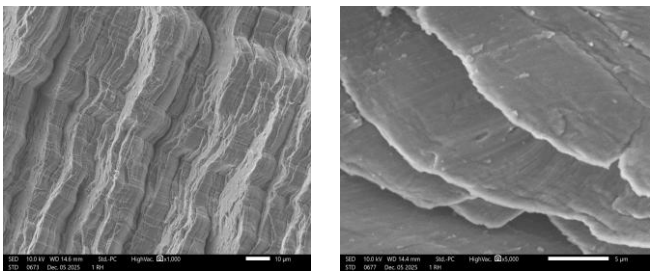

(a) (b)

Figure 5. SEM micrographs of the "middle 1" sample obtained at magnifications of: (a) – ×1000; (b) – ×5000

Based on the study of the vertical Al–V–Ti gradient along the ingot height, it was established that the absence of a pronounced vertical chemical gradient in the major alloying elements (Ti, Al, V) indicates the high efficiency of triple VAR remelting. This process ensures deep homogenization of the molten metal and effective suppression of segregation phenomena. As a result, the stability of the phase composition, the uniformity of the *α*/*β* microstructure morphology, and the predictability of mechanical properties along the ingot height are significantly improved.

Quantitative SEM–EDS data confirm the absence of a chemical gradient:

1). In all three "metallic" regions (top, bottom, and middle 1), the vanadium content lies within a narrow range of approximately 9.3-9.9 wt.%, indicating that a vertical V gradient along the ingot height is practically absent and that the β-stabilizer is distributed uniformly.

2). The aluminum content ranges from 2.5 to 3.1 wt.% across all three regions, with no significant vertical Al segregation detected.

3). A slight increase in titanium content from the top toward the middle 1 region was observed; however, this variation falls within the measurement uncertainty.

Thus, it was established that, with respect to the main alloying elements (Ti, Al, V), the ingot is chemically homogeneous along its height, and the VAR regime provides an acceptable level of macrosegregation control. The concentrations of Ti, Al, and V, the principal alloying elements in Ti-10V-2Fe-3Al, do not change significantly between samples taken from the top, middle 1, middle 2, and bottom regions of the ingot.

A compositional scatter of ≤1-1.5% is considered an excellent indicator of VAR melt quality. This level of scatter indicates minimal concentration differences: Al variations within ±0.5-1.0%, V variations within ±0.5-1.0%, and a stable Ti fraction of approximately 83-86%. For large industrial ingots with a mass of 4.5 t, such a low degree of compositional variation is regarded as a highly favorable result.

3.2.2. Results of vertical gradient analysis

An analysis of the vertical Al–V–Ti gradient along the ingot height revealed that the absence of a pronounced vertical chemical gradient in the main alloying elements (Ti, Al, V) indicates the high efficiency of triple vacuum arc remelting. This process provides deep homogenization of the molten metal and effectively suppresses macrosegregation. As a result, enhanced phase stability, uniform α/β microstructure morphology, and predictable mechanical properties along the ingot height are achieved.

The absence of a significant chemical gradient is confirmed by quantitative SEM–EDS results:

1) Vanadium (V). In all three metallic regions (top, bottom, and middle 1), the vanadium content falls within a narrow range of approximately 9.3–9.9 wt.%, indicating that a vertical V gradient is practically absent and that the β-stabilizer is distributed uniformly.

2) Aluminum (Al). The aluminum content ranges from 2.5 to 3.1 wt.% across all regions, with no evidence of significant vertical Al segregation.

3) Titanium (Ti). A slight increase in Ti content from the top toward the middle 1 region is observed; however, this variation lies within the measurement uncertainty.

Thus, the ingot is chemically homogeneous with respect to the principal alloying elements (Ti, Al, V) over its entire height, and the applied VAR regime provides acceptable macrosegregation control. The concentrations of Ti, Al, and V, the key alloying elements in Ti-10V-2Fe-3Al, do not change significantly across the top, middle 1, middle 2, and bottom regions.

A compositional scatter of 1-1.5% or less is considered an excellent indicator of VAR melting quality. This level of scatter corresponds to minimal elemental variations: Al within ±0.5-1.0%, V within ±0.5-1.0%, and a stable Ti fraction of approximately 83-86 wt.%. For large industrial ingots weighing 4.5 t, such a low degree of compositional variation represents an optimal result.

3.2.3. Development of an electrode quality control method based on SEM–EDS profiles

The obtained distribution profiles of V, Fe, Al, and O along scanning lines in the "top", "middle 1", "middle 2", and "bottom" regions make it possible to propose a quantitative electrode quality criterion based on microsegregation parameters:

– maximum deviation of β-stabilizer concentration (V, Fe) from the mean value along the line, $\Delta C_{\max}$;

– root-mean-square deviation σ_C along the line length;

– correlation length L_{corr} (the characteristic scale of chemically inhomogeneous regions);

– relative oxygen enrichment in locally enriched zones, $\Delta C_{O(local)}$.

In regions typical of the ingot middle, ΔC_{max} and σ_C remain limited, while L_{corr} is small, indicating fine-scale, well-averaged microsegregation. In the bottom part of the ingot, these parameters increase, reflecting the presence of larger-scale chemical inhomogeneities.

It is proposed to introduce an integral chemical inhomogeneity index, I_{chem}, that incorporates contributions from β-stabilizers and oxygen, and to define a limiting value, I_{chem}^{crit} (Critical Chemical Inhomogeneity Index). Exceeding this threshold indicates an unacceptable level of chemical inhomogeneity, at which the alloy or electrode should be rejected, or the triple-VAR remelting regime should be adjusted.

This approach transforms SEM–EDS analysis from a qualitative tool into a quantitative method for controlling ingot acceptance. Incorporating SEM–EDS-based homogeneity criteria into charge preparation regulations makes it possible to close the process loop "briquette → electrode → ingot" and to ensure reproducible microstructural quality under industrial production conditions.

4. Conclusions

It was established that the central regions ("middle 1") exhibit the most homogeneous distribution of V, Al, and Fe. The scatter of local β-stabilizer concentrations across the cross-section is minimal, reflecting a steady-state melting and solidification regime during triple VAR processing. The α-phase morphology in these regions is close to equilibrium: α colonies exhibit comparable thickness and length, while the β matrix forms a continuous framework without pronounced dendritic segregation.

Thus, for the first time, a comparative analysis of the α/β microstructure morphology along the height of an industrial electrode weighing 4500 kg produced by VAR at UKTMP has been performed.

It was demonstrated that no vertical chemical gradient exists along the electrode height, indicating the high quality and efficiency of the triple VAR process, as well as a uniform distribution of Al, V, and Fe governed by melting regimes and charge-mixing characteristics. The applied triple VAR technology ensures chemical homogeneity of the Ti-10V-2Fe-3Al alloy matrix along the ingot height. Local oxygen-enriched zones were identified, which may be used to predict a reduction in ductility and the potential formation of the α_2 phase.

Based on the results, a quality control methodology for electrodes was developed using SEM–EDS profiles.

Author contributions

Conceptualization: ATM, TAC; Data curation: ATM, BM; Formal analysis: ATM, TAC; Funding acquisition: ATM, TAC; Investigation: ATM, TAC; Methodology: ATM, TAC, BM; Project administration: ATM, TAC; Resources: ATM, TAC, BM; Software: ATM, TAC; Supervision: ATM, TAC, BM; Validation: ATM, TAC, BM; Visualization: ATM, TAC, BM; Writing – original draft: ATM, TAC, BM; Writing – review & editing: ATM, TAC, BM. All authors have read and agreed to the published version of the manuscript.

Funding

This research was carried out with the financial support of the agreement № 1090-TMK from 02.11.2025 / 11-168 from 19.11.2025. of Ust-Kamenogorsk Titanium and Magnesium Plant JSC.

Acknowledgements

The authors express their sincere gratitude to the editor and anonymous reviewers for their constructive comments and valuable suggestions, which have significantly improved the quality of this manuscript.

Conflicts of interest

The authors declare no conflict of interest.

Data availability statement

The original contributions presented in this study are included in the article. Further inquiries can be directed to the corresponding author.

References

[1] Banerjee, D., & Williams, J.C. (2013). Perspectives on titanium science and technology. *Acta Materialia, 61(3),* 844-879. https://doi.org/10.1016/j.actamat.2012.10.043

[2] Lutjering, G., & Williams, J.C. (2007). Titanium. *Springer.* https://doi.org/10.1007/978-3-540-73036-1

[3] Peters, M., Kumpfert, J., Ward, C.H. & Leyens, C. (2003). Titanium alloys for aerospace applications. *Advanced Engineering Materials, 5(6),* 419-427. https://doi.org/10.1002/adem.200310095

[4] Ballor, J., Li, T., Prima, F., Boehlert, C.J., & Devaraj, A. (2023). A review of the metastable omega phase in beta titanium alloys: the phase transformation mechanisms and its effect on mechanical properties. *International Materials Reviews*, *68*(1), 26-45. https://doi.org/10.1080/09506608.2022.2036401

[5] Yang, Z., Kou, H., Li, J., Hu, R., Chang, H., & Zhou, L. (2011). Macrosegregation behavior of Ti-10V-2Fe-3Al alloy during vacuum consumable arc remelting process. *Journal of Materials Engineering and Performance*, *20*(1), 65-70. https://doi.org/10.1007/s11665-010-9645-x

[6] Tahara, M., Hasunuma, K., & Hosoda, H. (2021). Microstructure of α+ β dual phase formed from isothermal α ″phase via novel decomposition pathway in metastable β-Ti alloy. *Journal of Alloys and Compounds*, *868*, 159237. https://doi.org/10.1016/j.jallcom.2021.159237

[7] Zhou, Z., Xiang, Z., Wang, B., Li, J., Chen, J., & Chen, Z. (2025). Influence of heat treatment on the mechanical properties, microstructure, and strengthening mechanisms of a novel metastable β titanium alloy. *Journal of Alloys and Compounds*, *1022*, 178726. https://doi.org/10.1016/j.jallcom.2025.178726

[8] Boyer, R.R. (1996) An Overview on the Use of Titanium in the Aerospace Industry. *Materials Science and Engineering: A*, *213,* 103-114. https://doi.org/10.1016/0921-5093(96)10233-1

[9] Taylor, C.M., Abrego Hernandez, S.G., Marshall, M. & Broderick, M. (2018). Cutting fluid application for titanium alloys Ti-6Al-4V and Ti-10V-2Fe-3Al in a finish turning process. *Procedia CIRP, 77,* 441-444. https://doi.org/10.1016/j.procir.2018.08.279

[10] Wang, X., Li, F., Xu, T., Ma, X., Hou, B., Luo, L., & Liu, B. (2021). Microstructure and microhardness evolution of Ti-10V-2Fe-3Al alloy under tensile/torsional deformation modes. *Journal of Alloys and Compounds, 881,* 160484. https://doi.org/10.1016/j.jallcom.2021.160484

[11] Ellyson, B., Saville, A., Fezzaa, K., Sun, T., Parab, N., Finfrock, C., Rietema, C. J., Smith, D., Copley, J., Johnson, C., Becker, C. G., Klemm-Toole, J., Kirk, C., Kedir, N., Gao, J., Chen, W., Clarke, K. D., & Clarke, A. J. (2023). High strain rate deformation of aged TRIP Ti-10V-2Fe-3Al (wt.%) examined by in-situ synchrotron X-ray diffraction. *Acta Materialia*, *245*, 118621. https://doi.org/10.1016/j.actamat.2022.118621

[12] Zhao, Q., Sun, Q., Xin, S., Chen, Y., Wu, C., Wang, H., Xu, J., Wan, M., Zeng, W., & Zhao, Y. (2022). High-strength titanium alloys for aerospace engineering applications: A review on melting-forging process. *Materials Science and Engineering A, 845,* 143260. https://doi.org/10.1016/j.msea.2022.143260

[13] Zhu, E., Li, F., Zhao, Q., Yuan, Z., You, J., & Hashmi, A.F. (2025). Deformation behavior of metastable Ti-10V-2Fe-3Al alloy subjected to varying pre-strain levels: Mechanism and microstructural adaptations. *Journal of Alloys and Compounds, 1029,* 180798. https://doi.org/10.1016/j.jallcom.2025.180798

[14] Qi, L., Zhang, K., Qiao, X., Huang, L., Huang, X. & Zhao, X. (2020). Microstructural evolution in the surface of Ti–10V–2Fe–3Al alloy by solution treatments. *Progress in Natural Science: Materials International, 30(1),* 106-109. https://doi.org/10.1016/j.pnsc.2020.01.011

[15] Qi, L., Qiao, X., Huang, L., Huang, X., Xiao, W. & Zhao, X. (2019). Effect of cold rolling deformation on the microstructure and properties of Ti-10V-2Fe-3Al alloy. *Materials Characterization, 155,* 109789. https://doi.org/10.1016/j.matchar.2019.109789

[16] Qi, L., Qiao, X., Huang, L., Huang, X. & Zhao, X. (2019). Effect of structural stability on the stress induced martensitic transformation in Ti-10V-2Fe-3Al alloy. *Materials Science and Engineering A, 756,* 381–388. https://doi.org/10.1016/j.msea.2019.04.058

[17] Danard, Y., Poulain, R., Garcia, M., Guillou, R., Thiaudière, D., Mantrid, S., Banerjee, R., Sun, F. & Prima, F. (2019). Microstructure design and in-situ investigation of TRIP/TWIP effects in a forged dual-phase Ti–10V–2Fe–3Al alloy. *Materialia, 8,* 100507. https://doi.org/10.1016/j.mtla.2019.100507

[18] Brozek, C., Sun, F., Vermaut, P., Millet, Y., Lenain, A., Embury, D., Jacques, P. J., & Prima, F. (2016). A β-titanium alloy with extra high strain-hardening rate: Design and mechanical properties. Scripta Materialia, 114, 60-64. https://doi.org/10.1016/j.scriptamat.2015.11.020

Ti-10V-2Fe-3Al үш мәрте қайта балқытылған қорытпаның құрылымдық және технологиялық қасиеттерін зерттеу

А.Т. Мамутова[1], Т.А. Чепуштанова[2*], Б. Мишра[3]

[1]*Өскемен титан-магний комбинаты АҚ, Өскемен, Қазақстан*
[2]*Satbayev University, Алматы, Қазақстан*
[3]*Вустер политехникалық институты, Вустер, АҚШ*

**Корреспонденция үшін автор: t.chepushtanova@satbayev.university*

Аңдатпа. Мақалада Ti-10V-2Fe-3Al құрамды үш мәрте қайта балқытылған қорытпаны алу нәтижелері келтірілген. Аталған қорытпаға жүргізілген SEM–EDS талдауының нәтижелері ұсынылып, өнеркәсіптік электродтың биіктігі бойынша Ti-10-2-3 қорытпасының құрылымы анықталған. Алғаш рет салмағы 4.5 т болатын электродтың үш сипаттамалық аймағында – «жоғарғы», «орта 1», «орта 2», «төменгі» – *α*/*β*-фазалардың морфологиясы мен жергілікті химиялық құрамын тікелей салыстыру нәтижелері кешенді SEM–EDS талдауы негізінде алынды. Негізгі легирлеуші элементтер (Ti, Al, V) бойынша құйма биіктігі бойымен толық химиялық теңестірілгені және ВДП (вакуумды доғалық қайта балқыту) режимі макросегрегацияның қолайлы деңгейін қамтамасыз ететіні анықталды. Ti-10V-2Fe-3Al қорытпасындағы басты легирлеуші элементтер – Ti, Al және V концентрацияларының сынамалар арасында айтарлықтай өзгермейтіні көрсетілді. SEM–EDS талдауы нәтижелері элементтер концентрациясының шашырауы ≤1–1.5% шегінде екенін көрсетті, бұл ВДП балқытудың сапалы жүргізілгенінің көрсеткіші болып табылады; яғни элементтер концентрацияларындағы айырмашылықтар минималды: Al өзгерістері ±0.5–1.0%, V өзгерістері ±0.5-1.0%, ал Ti тұрақты түрде шамамен ~83-86% үлесті құрайды. Морфологиялық зерттеулер нәтижесінде *α*/*β*-құрылымның біркелкі қалыптасқаны, айқын бағаналы сегрегацияның жоқ екені анықталды. *α*/*β*-фазалар морфологиясын тікелей салыстыру нәтижелері SEM–EDS профильдері бойынша электродтардың сапасын бақылау әдістемесін әзірлеуге мүмкіндік берді.

Негізгі сөздер: *титан қорытпасы; вакуумды доғалық қайта балқыту; SEM–EDS талдауы; үш мәрте қайта балқыту; α/β-микроқұрылым; морфология.*

Исследование структурных и технологических свойств сплава тройного переплава Ti-10V-2Fe-3Al

А.Т. Мамутова[1], Т.А. Чепуштанова[2*], Б. Мишра[3]

[1]*АО Усть-Каменогорский титаномагниевый комбинат, Усть-Каменогорск, Казахстан*
[2]*Satbayev University, Алматы, Казахстан*
[3]*Вустерский политехнический институт, Вустер, США*

**Автор для корреспонденции: t.chepushtanova@satbayev.university*

Аннотация. В статье представлены результаты получения сплава тройного переплава состава Ti-10V-2Fe-3Al, представлены результаты SEM–EDS анализа данного сплава, определена структура сплава Ti-10-2-3 по высоте промышленного электрода. Впервые получены результаты прямого сопоставления морфологии *α*/*β*-фаз и локального химического состава в трёх характерных зонах электрода весом 4.5 т – «верх», «середина 1», «середина 2», «низ» на основе комплексного анализа SEM–EDS. Установлено, что по основным легирующим элементам (Ti, Al, V) слиток полностью химически выровнен по высоте, и ВДП-режим обеспечивает приемлемый уровень макросегрегации. Установлено, что концентрации Ti, Al, V (главные легирующие элементы в Ti-10V-2Fe-3Al) не меняются существенно между пробами. Определено, что SEM–EDS результаты проб показывают на разброс концентраций элементов ≤1–1.5%, что считается показателем качества проведенной ВДП плавки, процент разброса означает, что различия концентраций элементов минимальны: изменения Al – в пределах ±0.5-1.0%, изменения V – в пределах ±0.5-1.0%, Ti занимает стабильную долю ~83–86%. Результатами морфологических исследований установлено, что структура *α*/*β* сформирована равномерно, без выраженной колонной сегрегации. Результаты прямого сопоставления морфологии *α*/*β*-фаз позволили разработать методику контроля качества электродов по SEM–EDS-профилям.

Ключевые слова: *титановый сплав; вакуумно-дуговой переплав; SEM–EDS анализ; тройной переплав; α/β-микроструктура, морфология.*

Publisher's note

All claims expressed in this manuscript are solely those of the authors and do not necessarily represent those of their affiliated organizations, or those of the publisher, the editors and the reviewers.